View metadata, citation and similar papers at core.ac.uk
brought to you by CORE
provided by Elsevier - Publisher Connector

The allosteric transition of glucosamine-6-phosphate deaminase: the structure of the T state at 2.3 Å resolution

Eduardo Horjales[1]*, Myriam M Altamirano[2], Mario L Calcagno[2], Richard C Garratt[3] and Glaucius Oliva[3]

Background: The allosteric hexameric enzyme glucosamine-6-phosphate deaminase from *Escherichia coli* catalyses the regulatory step of *N*-acetylglucosamine catabolism, which consists of the isomerisation and deamination of glucosamine 6-phosphate (GlcN6*P*) to form fructose 6-phosphate (Fru6*P*) and ammonia. The reversibility of the catalysis and its rapid-equilibrium random kinetic mechanism, among other properties, make this enzyme a good model for studying allosteric processes.

Results: Here we present the structure of $P6_322$ crystals, obtained in sodium acetate, of GlcN6*P* deaminase in its ligand-free T state. These crystals are very sensitive to X-ray radiation and have a high (78%) solvent content. The active-site lid (residues 162–185) is highly disordered in the T conformer; this may contribute significantly to the free-energy change of the whole allosteric transition. Comparison of the structure with the crystallographic coordinates of the R conformer (Brookhaven Protein Data Bank entry 1dea) allows us to describe the geometrical changes associated with the allosteric transition as the movement of two rigid entities within each monomer. The active site, located in a deep cleft between these two rigid entities, presents a more open geometry in the T conformer than in the R conformer.

Conclusions: The differences in active-site geometry are related to alterations in the substrate-binding properties associated with the allosteric transition. The rigid nature of the two mobile structural units of each monomer seems to be essential in order to explain the observed kinetics of the deaminase hexamer. The triggers for both the homotropic and heterotropic allosteric transitions are discussed and particular residues are assigned to these functions. A structural basis for an entropic term in the allosteric transition is an interesting new feature that emerges from this study.

Addresses: [1]Instituto de Biotecnología, Universidad Nacional Autónoma de México (UNAM), PO Box 510-3, Cuernavaca, MOR 62271, Mexico, [2]Departamento de Bioquímica, Facultad de Medicina, Universidad Nacional Autónoma de México (UNAM), PO Box 70-159, Ciudad Universitaria, Mexico City, DF 04510, Mexico and [3]Instituto de Fisica de São Carlos, Universidade de São Paulo, São Carlos, SP 13590-970, Brazil.

*Corresponding author.
E-mail: horjales@ibt.unam.mx

Key words: aldose-ketose isomerase, allosteric enzyme, allosteric transition, entropic effects

Received: 3 December 1998
Revisions requested: 18 January 1999
Revisions received: 17 February 1999
Accepted: 24 February 1999

Published: 29 April 1999

Structure May 1999, 7:527–537
http://biomednet.com/elecref/0969212600700527

© Elsevier Science Ltd ISSN 0969-2126

Introduction

Allosteric proteins control many chemical and physicochemical processes that are essential to cell function [1]. They play a key role in metabolic regulation as well as in receptor response, gene expression, chaperonin-assisted protein folding and cell–cell communication. The regulation of the binding properties of an allosteric protein can be described as an equilibrium of two different conformational states: a state with low or zero affinity for substrates, defined as the T state, and a state with high affinity for substrates and activators, the R state. The transition from one conformer to the other involves conformational changes at the quaternary structural level, which promote local modifications in the tertiary structure of the monomeric units, resulting in altered ligand-binding properties. These concepts were introduced 35 years ago by Monod *et al.* [2], and a formal theory was proposed two years later (the Monod–Wyman–Changuex [MWC] model [3]). This model does not exclude effects resulting from induced fit on substrate binding, which necessarily involve alterations to elements of the tertiary structure. It accounts for both the sigmoidal substrate-binding curve observed in the case of positive homotropic cooperativity as well as the heterotropic effects caused by modulating ligands binding to allosteric sites. The MWC model is essentially an equilibrium model and its application to kinetic processes is possible under the assumption that the enzyme follows a rapid equilibrium, rather than steady-state kinetics. Under steady-state conditions even the simplest allosteric models produce equations of great complexity and of very limited practical use [4]. In this context, glucosamine-6-phosphate deaminase (GlcN6*P* deaminase, EC 5.3.1.10) from *Escherichia coli* represents a convenient model system for the study of the structural basis of allosteric regulation in enzymes. It catalyses the isomerisation–deamination of glucosamine 6-phosphate (GlcN6*P*) to form fructose 6-phosphate (Fru6*P*) and

Table 1

Diffraction data statistics.

	50 Å–3.0 Å	3.0 Å–2.6 Å	2.6 Å–2.4 Å	2.4 Å–2.30 Å
Multiplicity	2.8 (2.8)	2.9 (3.0)	3.0 (3.0)	3.0 (3.0)
Completeness [F/σ(F)>1]	98.5 (98.5)	98.7 (99.1)	98.6 (98.0)	98.6 (98.6)
Completeness [F/σ(F)>2]	96.3 (96.3)	95.9 (95.2)	95.4 (93.6)	95.3 (95.0)
I/σ(I)	21.1	4.1	2.3	1.6
Rmerge(I)	4.1	19.2	32.3	43.0
Unique reflections [F/σ(F)>1]	14,024	21,344	26,995	30,597
Unique reflections [F/σ(F)>2]	13,706	20,735	26,135	29,545

Values given are the accumulated values; values in parentheses represent values for each resolution shell.

ammonia, following a rapid-equilibrium random mechanism [5–7]. The functional enzyme is hexameric (266 residues per monomer) and its activity is regulated in response to the binding of *N*-acetylglucosamine 6-phosphate (GlcNAc6*P*), the allosteric activator. Both homotropic cooperativity and GlcNAc6*P* activation of GlcN6*P* deaminase can be well explained in the framework of the MWC model [7]. GlcN6*P* deaminase behaves as a typical *K*-system enzyme (for a definition of *K* system see [3]) in which the allosteric activator binds exclusively to the R state. These properties are essential for the coordinated regulation of amino-sugar synthesis and utilisation in bacteria. Amino sugars are components of the bacterial cell wall, and they can be taken from the environment, when available, or synthesised from Fru6*P* and glutamine when the cells are grown in a minimal medium. In addition to its role in the genetic regulation of amino-sugar metabolism [8], GlcNAc6*P* is coinducer of a set of catabolic enzymes and corepressor of the GlcN6*P* synthase [8]. This metabolite is also an allosteric activator of GlcN6*P* deaminase, the enzyme promoting its conversion to a usable carbon source [6]. These regulatory mechanisms avoid a futile cycle of synthesis and deamination of GlcN6*P*.

We report here the three-dimensional structure at 2.3 Å resolution of GlcN6*P* deaminase in its ligand-free T conformer. We have previously published the structure of the R state of the same enzyme in the form of three different complexes, with both active and allosteric sites occupied

Table 2

Refinement procedure.

Stage number	Procedure	N step*	Res. (Å)	Initial R_{free}	Initial R	Final R_{free}	Final R	N ref.†	Scatters‡
1	Rigid minimisation	40	8–2.8	43.9	42.2	36.2	30.0	15,663	2092
2	Annealing								
	(Ti = 2000ºC)		8–2.3	41.6	37.1	39.8	33.9	29,090	2092
3	Minimisation	120	8–2.3	–	–	39.2	33.0	29,090	2092
4	B refinement	40	8–2.3	–	–	31.4	26.6	29,090	2092
5	sa/omap§ zero occupancy (residues163–184)		8–2.3	30.9	27.1	30.1	26.0	29,090	1907
5	sa/omap§ zero occupancy (residues 263–266)		8–2.3	30.8	26.5	30.4	25.8	29,090	2062
5	sa/omap§ zero occupancy (residues 163–184 & 263–266)		8–2.3	30.8	27.2	30.1	26.1	29,090	1877
5	Annealing similar to all 5		8–2.3	30.9	26.3	30.4	25.7	29,090	2092
	Number of zero occupancy atoms								
6	146 water molecules with B < 80. Positional	20	8–2.3	31.4	27.5	31.2	26.8	29,090	2238
	B refinement	20	8–2.3	30.8	26.4	25.8	21.3	29,090	2238
7	141 water molecules with B < 80. Positional and	20							
	B refinement	20	7–2.3	25.8	21.2	25.2	20.7	28,474	2233
8	Bulk-solvent and B refinement	10	100.–2.3	24.8	21.8	24.2	21.5	30,597	2233

*N step refers to the number of steps run in each minimisation (positional) or individual grouped B-factor refinements. †Stages 1–7: all measured reflections with F > 2σ and step 8: all measured reflections with F > σ). ‡Scatters refers to the number of non-hydrogen atoms included in the structure-factor calculation. After stage 5, there was good agreement between the model and the electron-density map. The density corresponding to amino acids 79–83, 162–183 and 263–266 was very weak, however. An omit-annealing procedure and a new map were then calculated excluding these regions from the phase calculation. No significant changes occurred and weak density was observed where the model had been placed. In spite of this observation, the lower or higher R_{free} and R values allowed us to decide which residues would be included in the phase calculations. Stage 6 started from the result of the annealing perfomed in stage 5 with full occupancy for all residues, as this had led to the most satisfactory results. These tests were performed at 2.3 Å resolution (43.0% for data from 2.4 to 2.3 Å on intensities). §Sa/omap is simulated annealing/omit map.

by ligands [9]. On the basis of these structures we describe a plausible mechanism for the allosteric transition of *E. coli* GlcN6*P* deaminase.

Results and discussion

Structure determination

Crystals of GlcN6*P* deaminase in its T state were obtained using sodium acetate as precipitant (see the Materials and methods section). The high solvent content of the crystals, 78%, may be correlated with their observed high sensitivity to radiation damage. A diffraction data set, 98.6% complete to 2.3 Å (Table 1), was measured at SSRL (Stanford Synchrotron Radiation Laboratory) and the structure was solved by molecular replacement using the monomer structure of the enzyme in its R state [9]. A unique solution for the rotation and translation functions was obtained using the program AMoRe [10], resulting in one molecule per asymmetric unit. The rotation function was calculated by including reflections from 20.0 to 4.0 Å, whereas in the translation function only the diffraction data from 8.0 to 4.0 Å were used. An R value of 36.1% and a correlation of 61.6 resulted from the translation-function calculation. The refined structure includes 141 water molecules per protein monomer and presents residuals of R = 20.7 and R_{free} = 25.2 (Table 2) and good departure from ideal geometry: 0.011 Å for distances, 1.5° for angles, 24.3° for torsion angles and 1.39° for impropers.

The structure of the T state

The crystal structure presents one monomer per asymmetric unit, which, due to the crystallographic symmetry, results in a hexameric arrangement with 32 internal symmetry, similar to the structure of the R state [9]. The enzyme in the present crystal form shows no ligand bound at either the allosteric or the active sites, thus confirming that it is the T-state conformer. The monomer fold is identical to that of the R state. It is an open α/β structure with a central seven-stranded β sheet surrounded by helices. In addition, a second three-stranded antiparallel β sheet is present. Between two of the strands of this second sheet there is a helix–loop motif that covers the active site as seen in the R conformer [9] termed the active-site lid (residues 163–183); this region shows the largest positional differences between the two conformers.

Figure 1

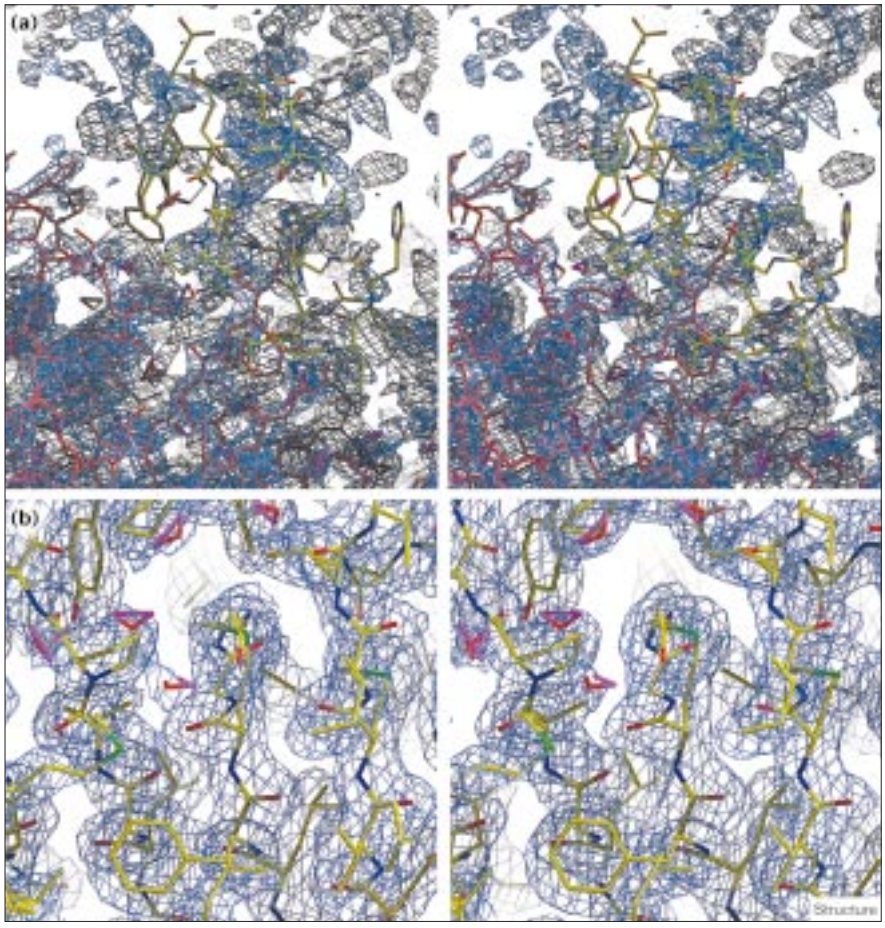

Two views of the electron-density map of GlcN6*P* deaminase in its T conformer. The maps were calculated using reflections up to 2.3 Å resolution and contoured at 1.0σ. (a) The active-site lid, which presents large B factors in the T conformer. Only weak density can be observed for residues 163–181 (coloured by atom type: carbons in yellow, nitrogens in blue, oxygens in red and sulphurs in green). In contrast, the rest of the structure (coloured red) presents good density. (b) View of the internal parallel β sheet, which shows the quality of the density for the majority of the structure.

Figure 2

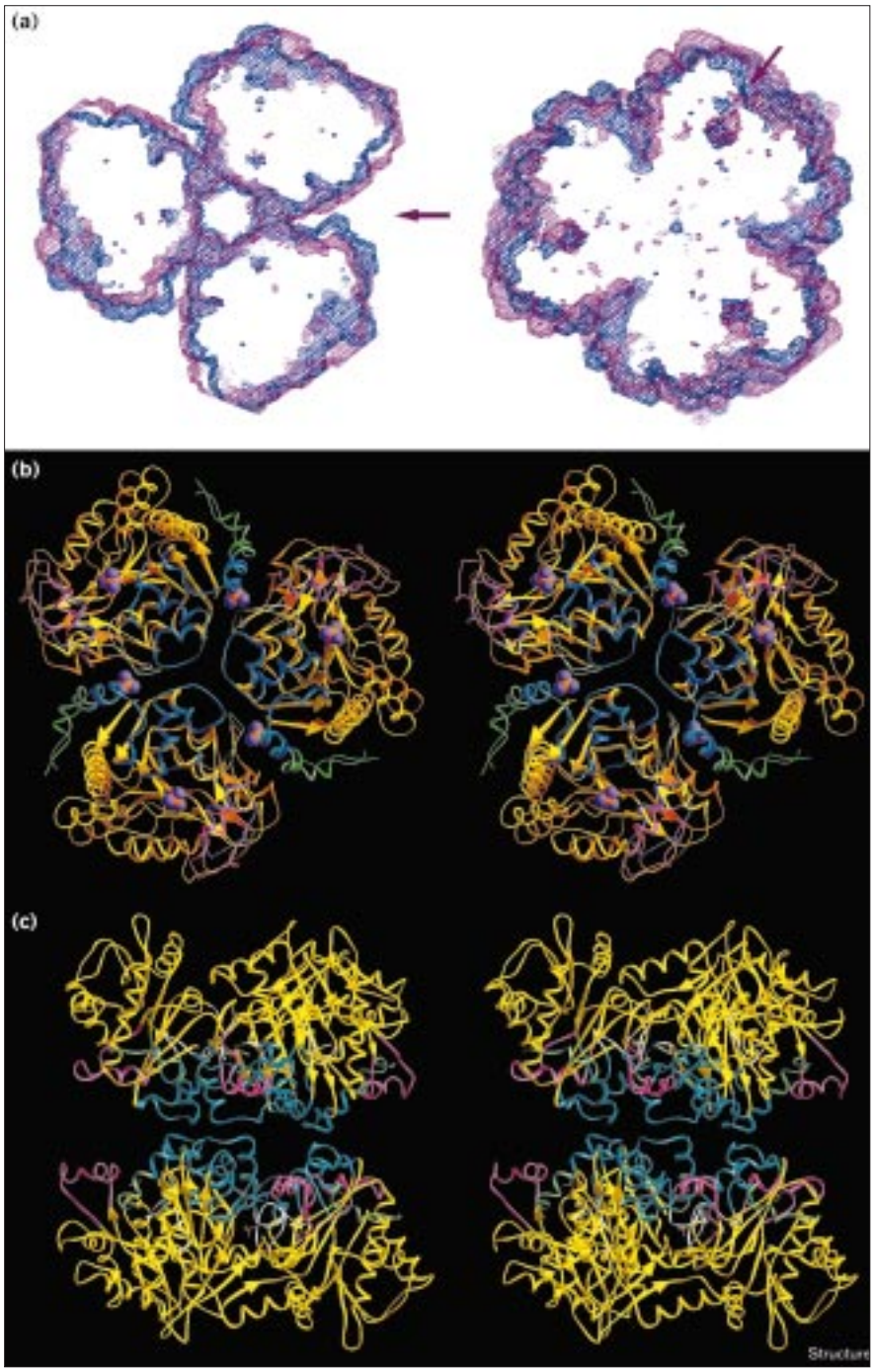

Comparison of the T and R crystallographic conformations. (a) Thin slabs of a mask that envelops each monomer are shown in the upper panels of the figure (T conformer in magenta, R in blue). Shown in the left panel is a section perpendicular to the threefold axis, which includes the allosteric site (indicated by the horizontal arrow). On the right, a section can be seen that includes the active site (indicated by the tilted arrow). In this case, the rotation of each monomer is difficult to observe because of the deformation of the active-site lid. A ribbon representation is presented in stereo pictures in the lower panels. (b) One of the trimers of the hexamer can be observed as viewed from the centre of the hexamer. The different structural modules (see below) are represented in different colours: the internal module in cyan, the external module in yellow, the active site lid in magenta, the loop formed by residues 144–154 in white and the C-terminal region (256–266) in green. The R conformer can be observed in darker colours. (c) The T conformer hexamer viewed along the twofold-symmetry axis. Colours are the same as in (b).

As this helix–loop motif is highly disordered in the T state (Figure 1), the observed differences in this region reflect the high flexibility of this part of the molecule rather than specific allosterically induced conformational changes. This suggests the existence of an entropic cost associated either with substrate binding or the allosteric quaternary change, which will be discussed later. On the other hand, the main difference in conformation between R- and T-state conformers is present at the active site, which presents a more open conformation at the T state.

The allosteric conformational change

Rigid-body superposition of the T- and R-state hexamers leads to a root mean square deviation (rmsd) of 4.7 Å, indicative of a large distortion during the allosteric transition. Starting from superposed hexamers, superimposition

Figure 3

The allosteric site observed in the same orientation for (a) the T conformer and (b) the R conformer.

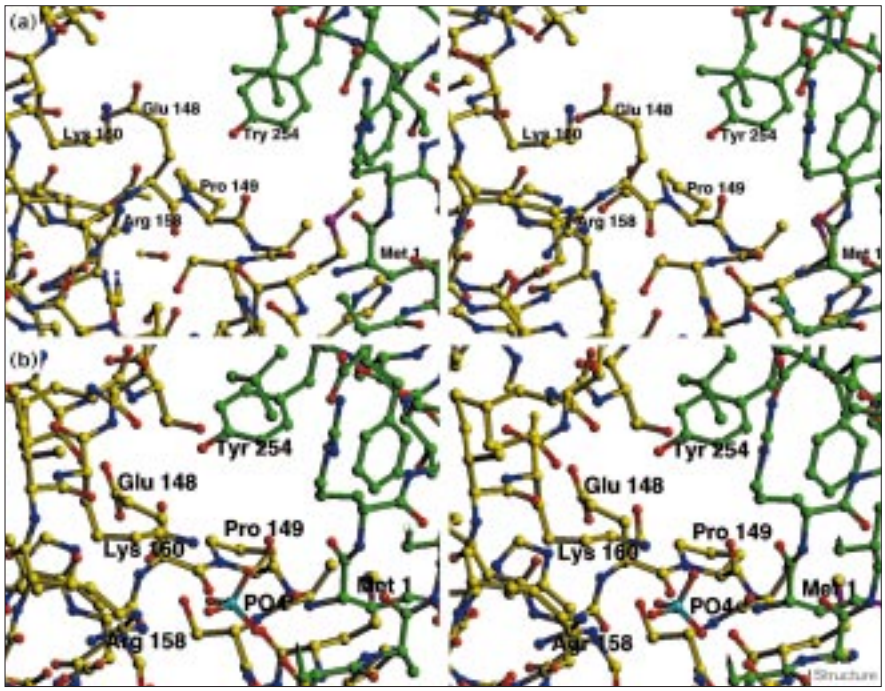

of an individual monomer from the R-state structure on its T-state equivalent (using all Cα atoms) shows that each monomer within the hexameric particle has rotated by an angle of 13.1° about a unique axis. These rotational axes lie approximately parallel to the threefold axis of the hexamer and pass close to residue 197 in each monomer. The concerted movement preserves the symmetry of the hexamer but leads to alterations in the relative orientations of the subunits, namely to the details of the quaternary structure of the particle. The rmsd of this monomer–monomer superposition is 1.06 Å, a value that is too large to be simply the result of errors in the structure determination itself. This indicates that the monomers do not move as rigid bodies but that the changes observed in the quaternary structure of the hexameric particle are accompanied by distortions to the tertiary structure of each individual monomer during the allosteric transition. Important to the analysis of this transition is the identification of the intermonomeric contacts within the oligomeric particle. The hexamers in both conformers present intermonomeric interactions that are limited to three regions: one close to the threefold axis, via residues 216–232 of each monomer, a second close to the twofold axis, including residues 244–250, and a third at the allosteric site itself, which lies between subunits related by the threefold axis and is spatially close to regions one and two.

The conformational change within the monomer can be described as a movement of two rigid bodies, the internal and external modules (Figure 2b and c). The internal module is responsible for most of the intermonomeric contacts of the hexamer and is composed of three segments: a helix–loop–helix motif (residues 207–233) that holds together the hexamer close to the threefold axis, a loop that establishes the intermonomeric contacts close to the twofold axis (residues 244–253) and a turn that is hydrogen-bonded to these structures (residues 137–143). The remainder of the structure forms the external module, with the exception of the loop formed by residues 144–154 and those residues that are highly disordered in the T conformer, as revealed by B factors greater than 50 Å^2. On undergoing the allosteric transition, the internal module must rotate 5.6° about an axis unique to the given subunit. These six internal modules, clustered around the threefold axis, form what we term the core of the hexamer and are responsible for the intersubunit contacts. On the other hand, the external module, which represents the greater part of each monomer, is more free to move during the allosteric transition as it is responsible for few intermonomeric contacts in either conformer. Those that do exist are located at the allosteric site and drastically change as a result of the transition, which may be described by a rotation of 13° in the case of the external module. The loop containing residues 144–154 undergoes an internal conformational change and cannot be included as part of either the internal or external modules. This loop constitutes the most direct contact between the allosteric and active sites, containing important residues for both allosteric activator binding and catalytic activity.

Figure 4

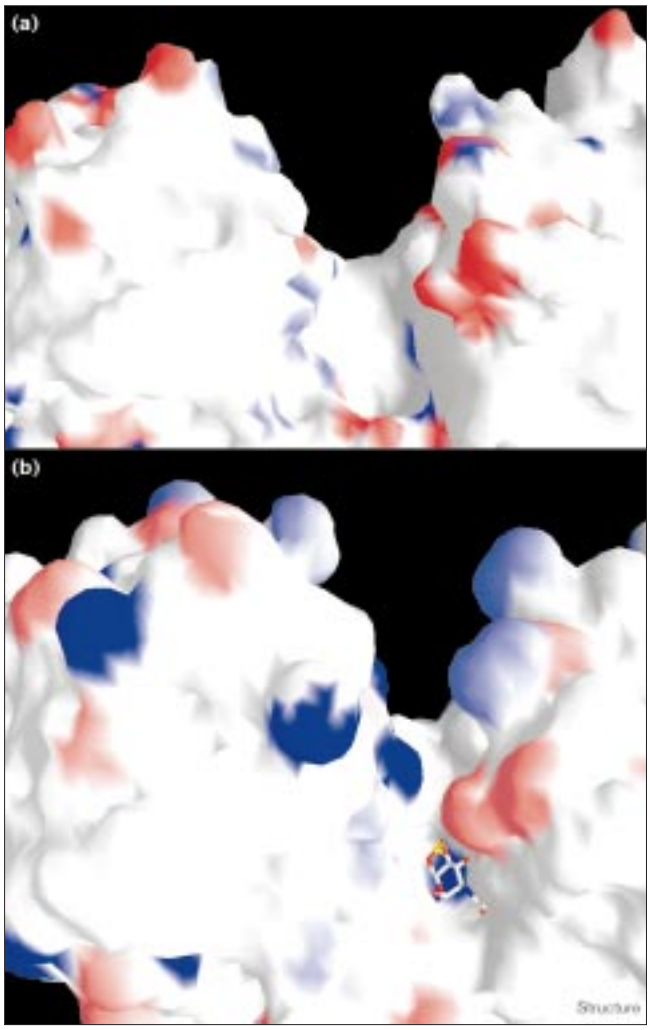

Electrostatic charges on the surface of (a) the T- and (b) the R-state conformers' intermonomeric interface. The activator was excluded from the charge calculation in the R conformer but it is represented in the figure. The concentrated blue spot around the activator in the R conformer is the result of its exclusion in the charge calculation. A region of positive charges (blue) expected to attract negative charges is observed in the intermonomeric region, whereas the rest of the molecule presents an overall negative charge (red). The wider intermonomeric cleft in the T conformer is also evident.

The allosteric site: heterotropic activation

The allosteric site, which is located at one of the intermonomeric interfaces and which securely accommodates the activator when the enzyme is in the R state, is entirely disrupted in the T-conformer structure (Figure 3). The mainchain nitrogen from Ser152 and the positively charged residues Arg158 and Lys160 of one monomer, together with the terminal amino group of the neighbouring subunit, bind the phosphate moiety of the allosteric activator in the R conformer [9]. In contrast, the terminal amino group in the T conformer lies more than 10 Å from the charged groups of residues Lys158 and Arg160 and is instead hydrogen-bonded to the carbonyl oxygen from Ala150 of the neighbouring monomer (Figure 3). The intermonomeric interface at the activator-binding site is wider in the T state than in the R state and a large net positive charge is evident in this region of the protein surface (Figure 4), which is neutralised, at least partially, upon activator or inorganic phosphate binding to the R state. The electrostatic repulsion among these charges might be partly responsible for favouring the open conformation of the allosteric site in the T state, similar to the mechanism involved in the stabilisation of one of the allosteric conformers of haemoglobin [11]. Another important intermonomeric contact present in this region involves Tyr254 (Figure 3). In both conformers the sidechain hydroxyl of Tyr254 forms an intersubunit hydrogen bond with its neighbouring monomer. However, whereas in the R conformer this interaction occurs with the carbonyl oxygen of Thr161, in the T state this is substituted by that of Pro149. Tyr254 has been proposed, from kinetic studies of mutant forms of the enzyme, to be a molecular switch that stabilises both the T- and R-state conformers, disfavouring possible intermediates along the trajectory of the allosteric transition [12,13]. The refined structure of the T conformer, together with the kinetic data, gives support to this hypothesis.

As described previously, Glu148 (Figures 3 and 5) participates in a proton-relay system that serves to polarise His143. This histidine is essential for the catalytic ring opening of the GlcN6*P* substrate. In the T state, however, Glu148 forms a salt bridge with Lys160 and a hydrogen bond with Arg158, the two basic residues described above as being essential for stabilising the charge on the phosphate group of the allosteric activator when bound to the R-state conformer. This requires a large change to the conformation of the sidechain of Glu148, which is almost certainly coupled to the observed deformation of the loop composed of residues 144–154. This is one of the few segments of mainchain that is highly ordered in both conformers but presents a non-rigid deformation upon undergoing the allosteric transition. It is central to the communication between the allosteric and active sites, as described in the following section.

The active-site region

In the absence of its allosteric activator, the enzyme displays an intense homotropic cooperativity. Although fitting kinetic data to MWC equations suggests that the T form of the enzyme is able to bind GlcN6*P* with low affinity [6,7], the geometry of the active site in the ligand-free T conformer shows an open conformation that cannot bind the substrate with similar contacts to those described for the structure of the R conformer [9]. In order to bind the phosphate group of the GlcN6*P* substrate via a salt bridge to Lys208 and three hydrogen bonds to the loop

Figure 5

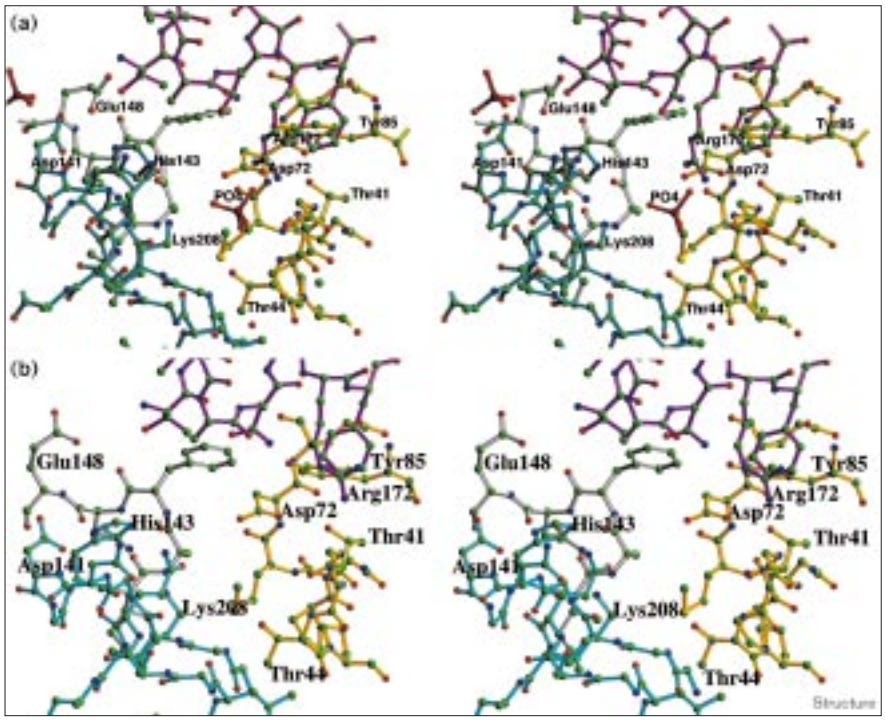

Stereo picture of the active site in both conformers: (a) R conformer, (b) T conformer. The various structural modules converge at the different parts of the active site, as shown by the different colour codes. Residues from the external module are shown in yellow, from the internal module in cyan, from the active-site lid in magenta and from the loop composed of residues 144–154 in white. The external module is in the same orientation in both conformers. The active-site lid has been displaced to build a narrower active site in the R conformer. The internal module is also in a slightly different orientation, rotating clockwise and approaching the observer, during the transition from the T to the R conformer.

formed by residues 41–44, the conformation of the binding region must change from the open geometry of the T state to the more closed conformation characteristic of the R state (Figure 5). This conformational change must proceed through a modification of the mainchain conformation of secondary structural elements (helix 205–216 and the β strand and helix close to loop 41–44, which can then trigger the concerted conformational change to the quaternary structure. Cocrystallisation of the enzyme in identical conditions to those used to obtain crystals of the T state, but in the presence of the competitive inhibitor (GlcN-ol-6*P*) or the allosteric activator (GlcNAc6*P*) or even the product (Fru6*P*), always results in crystals of good quality that present the enzyme in its R state. On the other hand, although soaking T-state crystals with 10^{-4} M competitive inhibitor GlcN-ol-6*P* results in no loss in diffraction quality, the ligand is not found in either the active or the allosteric site (E Rudiño-Piñera, S Morales-Arrieta, S Rojas and EH, unpublished results). This result indicates that the conformational change associated with enzyme–ligand binding in solution is hindered by crystal contacts that are distant from the active site, thus suggesting that the whole monomer is involved in the conformational change associated with substrate binding, consistent with the movement of the internal and external modules described above.

An important local conformational change relating allosteric control to catalysis is centred on residue Glu148. In the R conformation this glutamic acid participates in a special proton-relay system, where together with Asp141 it serves to both orient and polarise the imidazole ring of His143. This relay system catalyses the initial ring-opening step of the reaction. In the T structure Glu148 presents a drastically different conformation, with its sidechain carboxylate directed towards Lys160 in the allosteric site in a position 8.0 Å from the $N_{\delta 1}$ atom of His143.

Thus, the allosteric conformational change not only involves the relative movement of the internal and external modules, but it also requires a delicate electrostatic regulation. In the T state, Glu148 neutralises the positive charges at the allosteric site whereas in the R state this role is played by the phosphate group on the allosteric activator and Glu148 is free to fold into the active site, completing the proton-relay system necessary for catalysis.

As such, the loop formed by residues 144–154 plays a role as a linker in two different ways: linking the active site to the allosteric site and uniting the internal and external modules of each subunit.

The forces driving the transition and the mechanism of allosteric activation

The allosteric transition from T to R is generated upon binding of GlcNAc6*P* at the allosteric site or binding of active-site ligands (GlcN6*P*, Fru6*P*, GlcN-ol-6*P*). Crystals grown in phosphate as well as in ammonium sulphate have

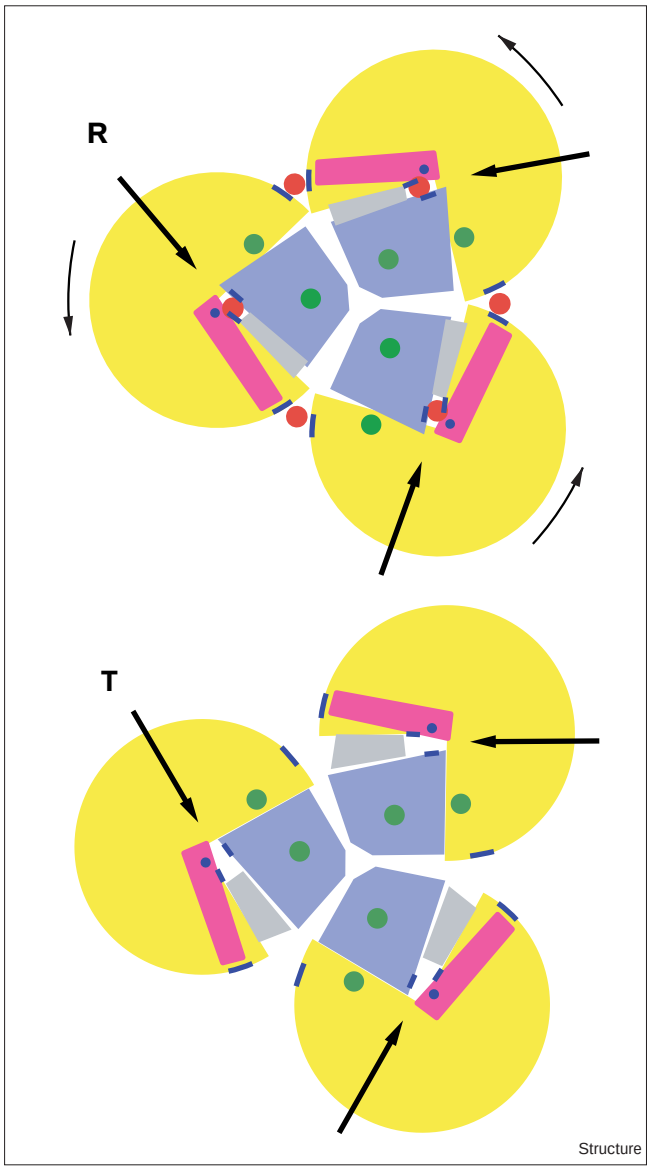

Figure 6

Structural components of GlcN6*P* deaminase and their movement during the allosteric transition. The internal module (in blue) presents a rigid anti-clockwise rotation of 5º around a centre close to the threefold axis (represented by the green dot in the blue region) during the transition from T to R. All the intersubunit contacts either connect these internal modules or are placed at the allosteric site (red dot at the intersubunit interfaces). The external module (in yellow) presents a larger anti-clockwise rotation of 13º around a centre laterally located in this structure (also represented by a green dot.) Positively charged residues (dark-blue dots and lines) at the active and allosteric sites are important for the allosteric mechanism and are responsible for the electrostatic forces driving the transition; the repulsion stabilises the T form of the enzyme, whereas the presence of the negatively charged effectors stabilises the R conformation. The active-site lid (in magenta), which is well positioned in the R conformer but highly disordered in the ligand-free T conformer (see text), may be related to entropic terms associated with the transition. The active-site lid connects the active and the allosteric sites; it is anchored close to the allosteric site and binds the substrate at the active site (ligands are represented as red dots in the cartoon of the R conformer). The loop comprised of residues 144–154 (in grey) also connects the allosteric and the active sites and is non-rigidly deformed during the transition. The allosteric site is totally distorted in the T state in accordance with the observation that activators behave as exclusive binding ligands. In contrast, in the T state the active site presents a conformation that has similar geometry to, but is more open than the R structure (the black arrows represent the entrance to the active site). The rigid character of the rotations generates the same conformation for the R state when the transition is driven from the active site (via substrate binding) or from the allosteric site (via the binding of the activator GlcNAc6*P*). The figure is represented as observed from the centre of the hexamer.

the R-state structure [14,9], showing that high concentrations of these divalent ions bind at both sites (where indeed they can be seen in electron-density maps) and produce the allosteric transition in the same way as other effectors. Nonphosphorylated molecules such as GlcN, GlcN-ol or Fru, however, do not bind to either the active or allosteric sites. Thus, the forces driving the transition are primarily associated with phosphate binding. The allosteric transition induced by phosphate and sulphate ions is a consequence of the presence of positively charged residues that come from the internal and external modules and the active-site lid, and which contribute to the structure of the active site. A repulsive interaction is thus present in the T conformer amongst the internal module (Lys208), the lid (Arg172) and the external module (two NH mainchain dipoles from residues Gly43 and Thr44). The presence of the negative charge of the phosphate at the active site transforms this repulsion into an attraction that drives the allosteric transition generating the cooperative effect. This molecular device, an active-site allosteric trigger, transforms electrostatic energy into mechanical movement. Similarly, in the case of the heterotropic transition, the allosteric site, which is in the interface between two threefold-related monomers, exhibits a large excess of positive charge distributed on both neighbouring subunits. The presence of the negative charge of the phosphate at the allosteric site generates an attraction between the external modules of two neighbouring monomers. Once again it is the rigid character of the external module that is essential for generating the same conformation for the R state when the transformation is driven by forces applied to either one of two different regions of the molecule. Thus, the entire range of properties displayed by GlcN6*P* deaminase, those associated with the active site and the effector-binding site, as well as the global quaternary changes related to the allosteric transition (Figure 6), can be explained through a two-state model, which consists of the ligand-free T conformer described in this paper and the liganded R conformer previously reported [9]. We wish to emphasise the observation that the properties of the conformational change that leads to the modifications of the active-site geometry are the same whether promoted by substrate or effector binding.

In most allosteric proteins for which the structure of both T and R states are known at good resolution the allosteric

transitions also appear as a change in the quaternary structure that can be described as rigid-body rotations and translation of some subunits with respect to others. These concerted motions that affect the whole molecule are the molecular basis of the coupling between the active and allosteric sites, which are mediated by specific changes in the geometry of some critical components at the binding sites [15]. In some multidomain enzymes allosteric regulation is mainly exerted via displacements involving individual domains, as is the case in *E. coli* pyruvate kinase I, in which all three domains forming each subunit of the tetrameric enzyme undergo concerted rotations [16,17]. In *E. coli* phosphoglycerate dehydrogenase, a *V*-type allosteric enzyme (for a definition of *V*-system see [3]), flexible domain rearrangement has been considered as the basis for understanding its catalysis and regulation [18]. Other allosteric proteins such as GroEl undergo an allosteric conformational change based on coupled specific displacements of its three domains, rather than ostensible quaternary displacements of the subunits [19].

Although GlcN6*P* deaminase does not contain distinct structural domains, the monomers present discrete tertiary-structure changes that we describe above as the mutual displacement of two modules in each subunit. In addition to the geometric contribution to allosteric conformational change found in classic allosteric proteins, the GlcN6*P* deaminase R–T transition may also present an entropic component as a consequence of the high flexibility of the active-site lid in the T conformer, which attains a greater order in the R state. This change in mobility can be attributed exclusively to substrate binding or to both substrate binding and the allosteric transition and is an aspect of the energetics of the allosteric transition of GlcN6*P* deaminase that deserves further investigation. Recently, entropic effects have been characterised in several allosteric enzymes [20–23], and they were theoretically discussed many years ago by Cooper and Dryden [24] who suggested that selective pressure for regulation could have produced allosteric responses not only supported by changing the mean conformational states of the protein but also by the thermal fluctuations about this mean.

Biological implications

E. coli glucosamine 6-phosphate (GlcN6*P*) deaminase constitutes a useful kinetic and structural model for the study of the allosteric control of enzyme function. In the present article we describe the structure of the T conformer of the enzyme. We had previously reported the structure of this enzyme in its high-affinity conformation, the R state. The knowledge of the structure of the T conformer provided us with enough information to describe the allosteric transition. Conformational changes involving the quaternary structure as well as internal rearrangements to each monomer were observed. The conformational change involving the quaternary structure is the result of changes in the tertiary structure of each subunit, which is associated with substrate or allosteric activator binding. The conformational change from the T to the R conformer is described as the relative movement of two rigid entities within each monomer, resulting in a catalytically active conformation at the active centre. Moreover, a conformation able to bind effectors at the allosteric site is generated in the R conformer, but it is totally distorted in the T conformer. Two different triggering mechanisms for this change are proposed, one fired from the catalytic centre and the other from the allosteric site. These structural changes, which can be described as a geometric modification of the subunits that propagates in a concerted fashion to the whole hexamer, are common to most well characterised allosteric enzymes. Besides this, our results suggest that the allosteric transition involves differences between the two deaminase conformers that are not associated with conformational changes, but that rather affect atomic mobilities. These effects are localised in the lid closing the active centre. We propose that they are responsible for an entropic term that makes a significant contribution to the energetics of the T–R transition.

Materials and methods

Crystallisation and structure determination

E. coli GlcN6*P* deaminase crystallises in its T conformer in sodium-acetate solutions at 4°C or 20°C, from 1.0 M to 3.5 M salt, in the pH range from 6.5 to 8.5. The crystals belong to space group $P6_322$, with unit cell axes a = 129.81 and c = 139.11, resulting in a solvent content of 78%. The crystals used for diffraction-data collection were grown using the vapour-diffusion technique at 20°C in 10 µl drops containing 15 mg/ml protein, under the following conditions: 1.75 M sodium acetate, 100 mM HEPES pH 7.0. Under such conditions large crystals presenting the morphology of hexagonal prisms, reaching dimensions up to 0.7×2.2 mm after six months, could be grown.

Diffraction data were obtained at the Stanford Synchrotron Radiation Laboratory (Station 7–1) at 4°C. The crystals initially diffracted up to 1.9 Å resolution, but radiation decay during the data collection severely limited the use of the data in the highest-resolution shells. To compensate for the loss in diffraction power of the exposed region of the crystal, it was translated along its longest dimension after every 10 frames of 1° rotations, to bring a fresh portion of the sample into the X-ray beam. The final processing of 30 frames collected in this way resulted in a data set that is 96% complete to 2.3 Å resolution, with the measurement statistics shown in Table 1. Data were integrated using the program DENZO [25,26] and scaled using the programs SCALA and AGROVATA of the CCP4 package [27]. The structure was solved using the molecular-replacement method as implemented in AmoRe [10] using the monomer of the R conformer structure [9] (PDB entry 1dea) as the search model. The refinement procedure was carried out using the program X-PLOR [28] and the details are presented in Table 2.

The superposition protocol

The present structure was superimposed on that of the R conformer previously described [9] (PDB code 1dea). On superposition of the two hexameric structures using all Cα carbons, an rmsd of 4.7 Å was obtained. This overall superposition shows the existence of a core within the hexamers, which exhibits a geometry that is conserved to a greater

extent than that of the rest of the particle, yet still presents some small deformations (Figure 2a). This core is centrally located around the three-fold axis of the hexamer and is formed by the juxtaposition of what we term the internal modules of each of the six subunits. The fact that the geometry of the core is better preserved than the remainder of the structure upon undergoing the allosteric transition suggested that each monomer could be more realistically treated as two rigid bodies rather than one: the smaller internal module located in the interior of the hexamer and a larger external module (Figure 2). In order to define the residues that comprise each module more unambiguously, the following procedure was adopted.

Initially, one monomer in the T conformer was superimposed as a rigid body on its equivalent in the R conformer. This resulted in an rmsd of 0.78 Å for 222 Cα atoms (all Cα atoms with B factors larger than 50 Å^2 in one of the structures were excluded from the calculation – residues 75–83, 110–115, 161–184 and 261–266). This rmsd is too high to derive solely from experimental errors in atomic positions and must be due to the relative movement of the two modules. As the external module is the larger, it dominates the above superposition and can be objectively defined by the LSQ_IMPROVE procedure of the program O [29] by limiting the calculation to include only equivalent Cα atoms separated by less than 0.7 Å in the original superposition of rigid subunits. This procedure automatically filters out the residues that belong to the internal module, as these are necessarily less well superposed in the original superposition. This procedure resulted in an rmsd of 0.31 Å for a subset of 156 Cα atoms (corresponding to residues 1–73, 84–108, 116–136, 155–159, 185–206 and 234–243). Choosing a smaller distance (0.5 Å) generates many gaps of only one or two amino acids. Larger distances up to 2.0 Å resulted in the inclusion of some additional Cα atoms as extensions to the same sequence segments identified above but these do not include the main part of the internal module. Distances larger than 2.0 Å included all the Cα atoms of the monomer in the superposition. This rigid part of the structure includes most of the monomer but excludes all amino acids that present intermonomeric interactions conserved in both T and R conformers. It enables us to objectively define the external module. Apart from the Cα atoms with B factors larger than 50 Å^2, only three sequence segments are excluded from this external module. These are residues 137–154, 207–233 and 244–260. The first segment is a loop built of three contiguous turns, which connects the active site to the allosteric site. We found that the first five residues of this segment (residues 139–143), which constitute a turn structure, together with the main part of the other two sequence segments 207–227 and 244–253, conform to another quasi-rigid body (rmsd = 0.32 Å on comparing the R- and T-state structures). This second quasi-rigid body provides a formal definition of the internal module and, as expected, is responsible for most of the intermonomeric contacts that build the hexamer. Figures 1 and 2a were obtained using the program O [29]. In Figure 4, the program GRASP [30] was used to represent the charge density on the molecular surface at the intermonomeric interface. Ball-and-stick figures were obtained with the program RIBBONS [31], as were Figures 2b and 2c.

Accession numbers

The coordinates of the T conformer have been deposited in the Protein Data Bank with accession code 1cd5.

Acknowledgements

We thank Harvey Bialy for the critical reading of the manuscript. This research was supported by grants from CNPq and FAPESP (Brazil) and from PAPIIT-UNAM (IN201295, IN220896 and IN221096). We acknowledge Sonia Rojas for assistance in the crystallisation experiments and Laura I Álvarez-Añorve for assistance in enzyme purification. GO is an international scholar of the Howard Hughes Medical Institute. This work is based upon research conducted at the Stanford Synchrotron Radiation Laboratory (SSRL), which is funded by the Department of Energy, Office of Basic Energy Sciences. The Biotechnology Program is supported by the National Institutes of Health, National Center for Research Resources, Biomedical Technology Program and the Department of Energy, Office of Biological and Environmental Research.

References

1. Perutz, M.F. (1990). *Mechanisms of Cooperativity and Allosteric Regulation in Proteins.* Cambridge University Press, Cambridge, UK.
2. Monod, J., Changeux, J-P. & Jacob, F. (1963). Allosteric proteins and molecular control systems. *J. Mol. Biol.* **3**, 318-356.
3. Monod, J., Wyman, J. & Changeux, J-P. (1965). On the nature of the allosteric transitions: A plausible model. *J. Mol. Biol.* **12**, 88-118.
4. Ricard, J. & Cornish-Bowden, A. (1987). Co-operative and allosteric enzymes: 20 years on. *Eur. J. Biochem.* **166**, 255-272.
5. Midelfort, C. & Rose, I.A, (1977). Studies on the mechanism of *Escherichia coli* glucosamine-6-phosphate isomerase. *Biochemistry* **16**, 1590-1596.
6. Calcagno, M.L., Campos, P.J., Mulliert, G. & Suástegui, J. (1984). Purification, Molecular and Kinetic Properties of glucosamine 6-phosphate Isomerase (deaminase) from *Escherichia coli*. *Biochim. Biophys. Acta* **787**, 165-173.
7. Altamirano, M.M., Plumbridge, J.A., Horjales, E. & Calcagno, M.L. (1995). Asymmetric allosteric activation of *Escherichia coli* Glucosamine 6-phosphate deaminase produced by replacements of Tyr121. *Biochemistry* **34**, 6074-6082.
8. Plumbridge, J.A., Cochet, O., Souza, J.M., Altamirano, M.M., Calcagno, M.L. & Badet, B. (1993). Coordinated regulation of amino sugar-synthesizing and –degrading enzymes in *Escherichia coli* K12. *J. Bacteriol.* **175**, 4951-4956.
9. Oliva, G., Fontes, M.R.M., Garratt, R.C., Altamirano, M.M., Calcagno, M.L. & Horjales, E. (1995). Structure and catalytic mechanism of glucosamine 6-phosphate deaminase from *Escherichia coli* at 2.1 Å resolution. *Structure* **3**, 1323-1332.
10. Navaza, J. (1994). AMoRe: an automated package for molecular replacement. *Acta Crystallogr. A* **50**, 157-163.
11. Perutz M.F., Shih D.T. & Williamson D. (1994). The chloride effect in human haemoglobin: a new kind of allosteric mechanism. *J. Mol. Biol*. **239**, 555-560.
12. Altamirano, M.M., Hernández-Arana, A., Tello-Solís, S. & Calcagno, M.L. (1994). Spectrochemical evidences for the presence of a tyrosyl residue in the allosteric site of glucosamine-6-phosphate deaminase from *Escherichia coli*. *Eur. J. Biochem*. **220**, 409-413.
13. Montero-Morán, G.M., Horjales, E., Calcagno M.L. & Altamirano M.M. (1998). Tyr254 hydroxyl group acts as a two-way switch mechanism in the coupling of heterotropic and homotropic effects in *Escherichia coli* glucosamine-6-phosphate deaminase. *Biochemistry* **37**, 7844-7849.
14. Horjales, E., Garratt, R.C., Oliva, G., Altamirano, M.M. & Calcagno, M.L. (1992). Crystallisation and preliminary crystallographic studies of glucosamine-6-phosphate deaminase from *Escherichia coli. J. Mol. Biol*. **226**, 1283-1286.
15. Stevens, R.C. and Lipscomb, W.N. (1993). Allosteric Enzymes. In *Molecular Structures in Biology* (Diamond, D., Koetzle, T.F., Prout, K. & Richardson, J.S., eds), pp. 223-259, Oxford University Press, Oxford.
16. Mattevi, A. Rizzi, M. & Bolognesi, M. (1996). New structures of allosteric proteins revealing remarkable conformational changes. *Curr. Opin. Struct. Biol.* **6**, 824-829.
17. Mattevi, A., Valentini, G., Rizzi, M., Speranza, M.L, Bolognesi, M. & Coda, A. (1995). Crystal structure of *Escherichia coli* pyruvate kinase type I: molecular basis of the allosteric transition. *Structure* **3**, 729-741.
18. Schuller, D.J., Grant, G.A. & Banaszak, L.J. (1995). The allosteric ligand site in the V_{max}-type cooperative enzyme phosphoglycerate dehydrogenase. *Nat. Struct. Biol*. **2**, 69-76.
19. Ma, J. & Karplus, M. (1998). The allosteric mechanism of the chaperonin GroEL: a dynamic analysis. *Proc. Natl Acad. Sci. USA* **15**, 8502-8507.
20. Braxton, B.L., Mullins, L.S., Raushel, F.M. & Reinhart, G.D. (1996). Allosteric effects of carbamoyl-phosphate synthetase from *Escherichia coli* are entropy-driven. *Biochemistry* **35**, 11918-11924.
21. Luiu, L., Wales, M.E. & Wild, J.R. (1998). Temperature effects on the allosteric responses of native and chimeric aspartate transcarbamoylases. *J. Mol. Biol.* **282**, 891-901.
22. Tlapak-Simmons, V.L. & Reinhart, G.D. (1998). Obfuscation of allosteric structure-function relationships by enthalpy-entropy compensation. *Biophys. J.* **75**, 1010-1015.
23. Bucci, E., Gryczynsky, Z., Razynska, A. & Kwansa, H. (1998). Entropy-driven intermediate steps of oxygenation may regulate the allosteric behavior of hemoglobin. *Biophys J.* **74**, 2638-2648.
24. Cooper, A. & Dryden D.T. (1984). Allostery without conformational change: A plausible model. *Eur. Biophys. J.* **11**, 103-109.

25. Otwinowski, Z. (1993). Oscillation data reduction program. In *Proceedings of the CCP4 Study Weekend*: *Data Collection and Processing*. (Sawyer L., Isaacs, N. & Bailey S., eds), pp. 56-62, SERC Daresbury Laboratory, Warrington.
26. Otwinowski, Z. & Minor W. (1996). *Processing of X-ray Diffraction Data Collected in Oscilation Mode*. (Carter, C. & Sweet, R.M., eds), pp 307-325, Academic Press, Boston MA.
27. Collaborative Computational Project, Number 4, (1994). The CCP4 suite: programs for protein crystallography. *Acta Crystallogr*. *D* 50, 760-763.
28. Brünger, A.T. (1992). *X-PLOR Version 3.1. A System for X-ray Crystallography and NMR*., Yale University Press, New Haven, CT.
29. Jones, T.A., Zou, J.Y., Cowan, S.W. & Kjeldgaard, M. (1991). Improved methods for building protein models in electron density maps and the location of errors in these models. *Acta Crystallogr*. *A* 47, 110-119.
30. Nicholls, A., Sharp, K.A. & Honig, B. (1991). Protein folding and association: Insights from the interfacial and thermodynamic properties of hydrocarbons. *Proteins* 11, 281-296.
31. Carson, M. (1991) RIBBONS 2.0. *J. Appl. Crystallogr.* 24, 958-961

Because *Structure with Folding & Design* operates a 'Continuous Publication System' for Research Papers, this paper has been published on the internet before being printed (accessed from http://biomednet.com/cbiology/str). For further information, see the explanation on the contents page.